ACS OMEGA

http://pubs.acs.org/journal/acsodf

Article

Reduced Pollutant Emissions and Slagging Rate of Biomass Pellet Combustion by Optimizing the Multilayer Distribution of Secondary Air

Zhisen He, Shanjian Liu,* Shuaichao Wang, Weidong Liu, Yongjun Li, and Xiangdong Feng

Cite This: *ACS Omega* 2022, 7, 28962−28973

Read Online

ACCESS | Metrics & More | Article Recommendations

ABSTRACT: The utilization of coal and other fossil fuels is becoming increasingly restricted. Biomass, as a clean and renewable energy, plays a significant role in achieving zero carbon emissions. However, biomass is prone to slagging in the combustion process due to its high alkali metal content. The ash slagging rate and pollutant emission level of flue gas can be reduced by optimizing the air distribution, in order to decrease the fuel layer temperature in the combustion chamber. The results reveal opposite change trends of CO and NO_x concentrations in the flue gas. The NO_x emissions of corn stalk combustion under the multilayer secondary air distribution are obvious compared with those of rice husk combustion. The slagging rate of corn stalks is highly correlated with temperature T_1 of the fuel bed. The silica ratio (G), alkali/acid ratio (B/A), Na content index (Na (index)), and alkaline index (Al_c) cannot accurately predict the slagging tendency when temperature T_1 changes. Therefore, the modified predictive index (G_t) was proposed to predict the slagging tendency of corn stalks with the combustion zone temperature T_1 effectively. The experimental results can contribute to the efficient combustion and low pollutant emissions of biomass.

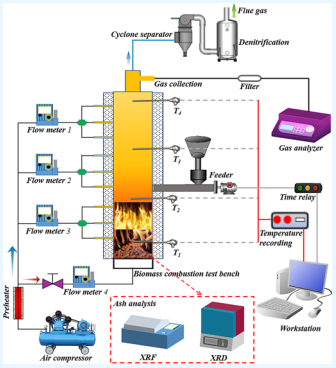

1. INTRODUCTION

Driven by the goal of carbon neutralization, the utilization of biomass energy has attracted a great amount of attention over recent years. Biomass is the only renewable carbon source that can used to produce a wide range of high-quality fuels, chemicals, and bio-based materials.[1−3] However, due to the limitation of different technologies, the large-scale utilization of straw biomass as an energy source is generally based on direct or indirect combustion. In particular, biomass pellet fuel is used widely at the commercial level, overcoming many limitations of raw biomass, such as low density, low calorific value per unit volume, and difficulties in efficient combustion.[4−6] Straw biomass typically contains a high content of alkali metals and ash.[7−9] Serious ash slagging and agglomeration often occur in the furnace during combustion, and the pellet fuel of straw biomass further increases the agglomeration degree of ash. This is mainly due to the dense structure of pellet fuel, which contains low-melting-point compounds that polymerize easily at high temperatures. A layer of glass-like melt is formed on the outer surface of straw pellet fuel, and the fuel is not fully burned inside. This prevents sufficient contact between fuel and combustion air. Difficulties in full combustion result in high pollutant emissions in flue gas as well as serious equipment corrosion and slagging complications.[10,11] Straw is the main byproduct of crop harvesting and has the advantages of a lower price, wide range of sources, and easier access compared to woody biomass. However, crop straw usage is typically inefficient, causing serious environmental pollution hazards to rural areas and towns.[12,13]

Previous research has investigated the pretreatment of straw-like biomass by pickling or alkaline washing,[14,15] adding additives that do not easily form slag,[16,17] and the co-combustion with coal, woody biomass, etc.[18,19] Such methods are able to effectively reduce the degree of slagging and agglomeration. In particular, local low-temperature combustion via a suitable air distribution is a simple, easy, and low-cost strategy for the reduction of straw biomass slagging. At present, air staged combustion technology is generally used in pulverized coal burners or circulating fluidized bed boiler systems.[20] Liu et al.[21] employed a 50 kW small household biomass pellet burner with two secondary air ducts of different heights (9 and 21 cm above the bed). The results revealed the significant reduction of NO_x emissions with the secondary air set at a higher position, while CO emissions were enhanced and the combustion efficiency was lowered. Thus, blindly increasing the secondary air proportion is not advisable; rather, it must be controlled adequately. Fan et al.[22] employed a 20

Received: April 26, 2022
Accepted: July 28, 2022
Published: August 8, 2022

ACS Publications

© 2022 The Authors. Published by American Chemical Society

kW pulverized coal reactor to conduct deep and medium air staged combustion tests. Under the air staged combustion of pulverized coal, the key combustion zone was in a state of insufficient air supply, resulting in a strong reducing atmosphere that inhibited the formation and production of NO during the combustion process. Therefore, the peak NO concentration in the key combustion zone exhibited a rapid drop. In addition, the deeper the classification degree, the lower the NO emission concentration. Sher et al.[23] burned three pellet fuels (straw, miscanthus, and peanut shells) in a 20 kW small bubbling fluidized bed (BFB) burner in order to evaluate the influence of the secondary air injection position on the emission concentration (NO_x, CO) and temperature distribution of the gas during fuel combustion. Increasing the excess air coefficient reduced CO concentrations and enhanced NO_x concentrations at the outlet. Injecting the secondary air at a higher point led to the majority of fuel combustion achieving a significant reduction in NO_x emissions.

There currently exist numerous applications of air-staged air distribution combustion technology for coal and biomass in large-scale combustion devices.[24−27] However, the majority of studies focus on fuel combustion characteristics, with typical equipment including tube furnaces, muffle furnaces, thermogravimetric analyzers, etc. Large differences between the operating conditions of the test equipment and the actual combustion device result in discrepancies between the data and conclusions and the actual fuel combustion in large furnaces. In order to overcome these limitations, we design a biomass pellet combustion test device with a multilayer secondary air distribution. The effects of different primary and secondary air (PA and SA) grading ratios and multilayer secondary air ratios on the concentration of CO, NO_x, and other pollutants in the flue gas and combustion efficiency are studied, and the corresponding variations of the combustion ash composition are analyzed. Effectively controlling the multilayer secondary air distribution lowers the NO_x and CO emissions from the combustion of corn stalk and rice husk pellets and increases the combustion efficiency. The results provide technical support for the reasonable combustion and air distribution of large-scale and domestic biomass combustion equipment.

2. MATERIALS AND METHODS

2.1. Multilayer Secondary Air Distribution Straw Biomass Combustion Test Bench. The structure of the biomass pellet combustion test bench with multilayer secondary air distribution is shown in Figure 1. The parameters of the designed biomass pellet combustion test bench are shown in Table 1. Nine secondary air ducts are evenly and symmetrically distributed along the height of the entire combustion chamber, and the distance between the upper and lower air ducts is 5 cm. The air ducts are divided into three groups along the height of the combustion chamber, denoted as the upper, middle, and lower secondary winds (US, MS, LS). The secondary air (room temperature) enters the combustion chamber at different heights and proportions. The upper, middle, and lower secondary air volumes are precisely controlled by the LZB-15 mass flow meter. The primary air (room temperature) passes through the grate into the combustion chamber, and the air volume is controlled by a 1000WOG valve. The air distribution at the bottom of the test bench is mainly achieved by the grate, which not only supports the material but also acts as an air distribution plate. The grate

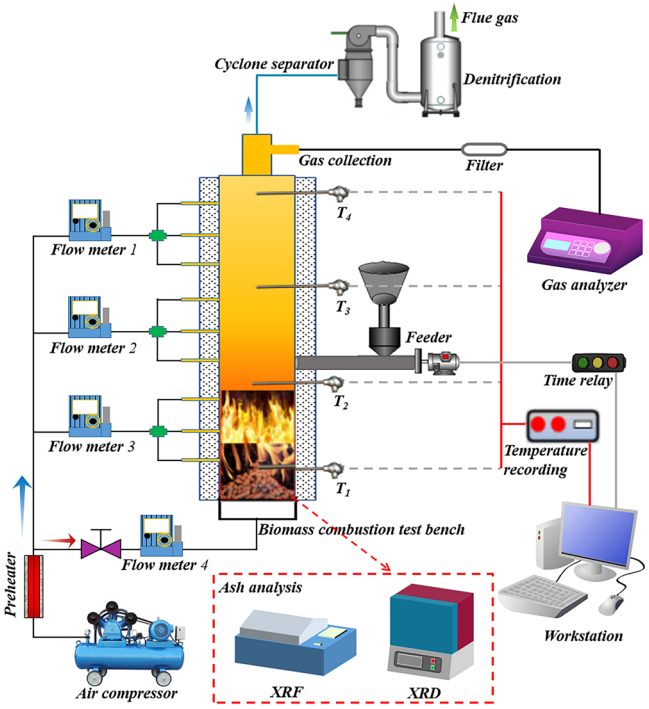

Figure 1. Test bench for burning straw biomass.

Table 1. Specific Parameters of Combustion Test Bed

parameters	values	parameters	values
design materials	corn stalks, rice husks	overall height	0.90 m
rated feeding volume	3.0 kg/h	combustion chamber volume	0.02 m^3
rated combustion efficiency	95%	secondary air duct spacing	3.0 cm
distance between adjacent temperature measuring ports	13.0 cm	combustion chamber diameter	0.20 m
design rated power	48 × 10^3 kJ/h	inner diameter of secondary air	5.0 mm

reasonably distributes the primary air supplied from the bottom of the furnace, so that the air distribution is more uniform and the combustion is more sufficient. In addition, a portion of the bottom slag is present at the bottom to act as a bed material when the test bench starts to maintain the initial material balance. The bed material is also present during the combustion process to maintain normal pressure in the furnace.

2.2. Analysis of Raw Material Characteristics. Rice husks and corn stalks are typical biomass available across the globe, with a huge annual output. Research has demonstrated that the burning of biomass is prone to problems such as high pollutant emissions and insufficient combustion.[28] The pellet fuel of rice husks and corn stalks are commonly employed in studies on pollutant emissions and slagging characteristics. The biomass molding pellets used in this study had a diameter of 8−10 mm and average length of 3−5 cm. Although the ash content of corn stalks is only half of that of rice husks, the fixed carbon content is twice as high (Table 2). There is little difference between the content of the key elements in the two raw materials, yet the nitrogen content of the corn stalks is

https://doi.org/10.1021/acsomega.2c02587
ACS Omega 2022, 7, 28962−28973

Table 2. Characteristic Analysis of Corn Stalks and Rice Husk Raw Materials on an As-Received Basis

	proximate analysis (wt%)				ultimate analysis (wt %)					
sample	moisture	volatiles	fixed carbon	ash	[C]	[H]	[O]	[N]	[S]	LHV (MJ/kg)
corn stalks	10.22	66.24	14.81	8.73	41.97	5.81	48.21	1.12	0.06	15.72
rice husks	6.31	71.09	7.69	14.91	39.22	5.51	49.9	0.34	0.08	15.43

Table 3. Inorganic Elemental Composition of Corn Stalks and Rice Husks

	elemental composition (wt %)									
sample	[Na]	[Mg]	[Al]	[Si]	[P]	[S]	[Cl]	[K]	[Ca]	[Fe]
corn stalks	0.060	0.313	0.194	3.090	0.167	0.201	0.838	3.180	1.230	0.222
rice husks	0.085	0.132	0.081	8.520	0.101	0.010	0.360	1.130	0.204	0.062

extremely high, reaching more than three times that of the rice husks.

Table 3 presents the results of the X-ray fluorescence spectrometry (XRF, Rigaku ZSX100e) of corn stalks and rice husks. Both the chlorine and potassium contents in rice husks and corn stalks are relatively high, and the high content of potassium is the main factor causing the slagging of biomass combustion.[29] Potassium content generally exists as K_2O, KOH, K_2SO_4, K_2CO_3, etc. in the ash. The melting points of these substances tend to be low. With the exception of a few compounds (e.g., K_2SO_4), the melting points of most substances are between 350 and 800 °C. In fact, at higher combustion temperatures, these may even be reduced by the carbon-hydrogen fuel matrix to metal vapor. These alkali species will readily react with the ubiquitous water vapor to more stable and relatively volatile hydroxides.[30] A large amount of hydroxides combined with the unburned coke pellets, resulting in problems including insufficient combustion and slagging. This causes serious harm to the biomass boiler. Note that the silicon contents in both rice husks and corn stalks are high, accounting for more than 40% of the total inorganic elements. The silicon content in the rice husks accounts for 90% of the total inorganic elements and has an important effect on the post-combustion ash composition of rice husks.

2.3. Combustion Efficiency (η_c). The combustion efficiency can reflect the combustion effect of fuels under different working conditions. The amount of fly ash discharged from the combustion chamber of biomass pellet fuel is relatively low, and thus only the heat loss caused by combustible gas and unburned carbon in the bottom ash is considered.

$$\eta_C = 100 - q_1 - q_2 \quad (1)$$

$$q_1 = 3.2\alpha\phi(\mathrm{CO}) \quad (2)$$

where η_c is the combustion efficiency, %; q_1 is the heat loss due to unburned gas, %; q_2 is the heat loss due to unburned carbon, %; α is the excess air coefficient; and $\varphi(\mathrm{CO})$ is the CO content in the flue gas, %.

For biomass combustion, the unburned carbon generally remains in the ash, and the formula of q_2 can be simplified as

$$q_2 = \frac{33727 A_{ar} C_Z}{Q_r(100 - C_Z)} \quad (3)$$

where A_{ar} is the ash content of the raw material received, %; C_z is the content of unburned carbon in the ash, %; and Q_r is the low calorific value of the raw material received, kJ/kg.

3. RESULTS AND DISCUSSION

3.1. Emission Law of Combustion Pollutants. In the fuel combustion process, the proper amount of air entering will have a great influence on the oxidation or reduction atmosphere of the combustion area and consequently affect the emission level of particulate matter, nitrogen oxide, and other pollutants. We employed rice husks and corn stalks as fuels to investigate the flue gas pollutant emissions and the combustion chamber temperature changes using the above biomass combustion test bench (Figure 1). All the combustion experiments were performed at a feeding rate of 1.5 kg/h biomass briquette. In order to mark the various air distribution conditions of the experiments, we propose a primary air application, with excess air coefficients of 1.1, 1.2, 1.3, and 1.4 (EAC1.1, EAC1.2, EAC1.3, EAC1.4, respectively). The primary and secondary air ratios are set as PA:SA = 70%:30% or 60%:40%, respectively. The secondary air enters the furnace from the upper, middle, and lower entrances (US, MS, LS), labeled US (30%), MS (30%), and LS (30%) or US (40%), MS (40%), and LS (40%), respectively. When the primary and secondary air ratios are PA:SA = 60%:40%, the lower, middle, and upper three layers of the secondary air are allocated according to the following proportions (1/2, 0, 1/2), (1/3, 1/3, 1/3), (0, 1/2, 1/2), and (1/2, 1/2, 0) and marked as W_1, W_2, W_3, and W_4, respectively. In order to compare with the fuel combustion case of the presence of just primary air, the following conditions are selected as the control groups. The experimental data of corn stalk pellet combustion condition EAC1.2 is used for control group (CG), while the experimental data of rice husk combustion condition EAC1.3 is also selected for control group (CG).

Figure 2 presents the variations of the NO_x and CO concentrations and combustion zone temperature T_1 of the rice husk pellet under different air distribution conditions. The NO_x emission concentrations at the combustion outlet are approximately 200−260 mg/m^3 when the excess air coefficient is 1.1, 1.2, 1.3, and 1.4. Moreover, the NO_x emissions during the staged combustion of the primary and secondary air range within 150−250 mg/m^3, which is lower than the non-staged combustion concentrations. Temperature T_1 under these working conditions is between 650 and 800 °C and increases with the excess air coefficient. This may be attributed to the high ash and silicon content in the rice husks, preventing the fixed carbon to fully burn out.[31] Consequently, the increase of excess air coefficient helps to burn out the rice husks. In addition, the thermocouple is located just above the fuel bed. Usually, this implies that the measured temperature is very sensitive to the exact position as well as process conditions in

https://doi.org/10.1021/acsomega.2c02587
ACS Omega 2022, 7, 28962−28973

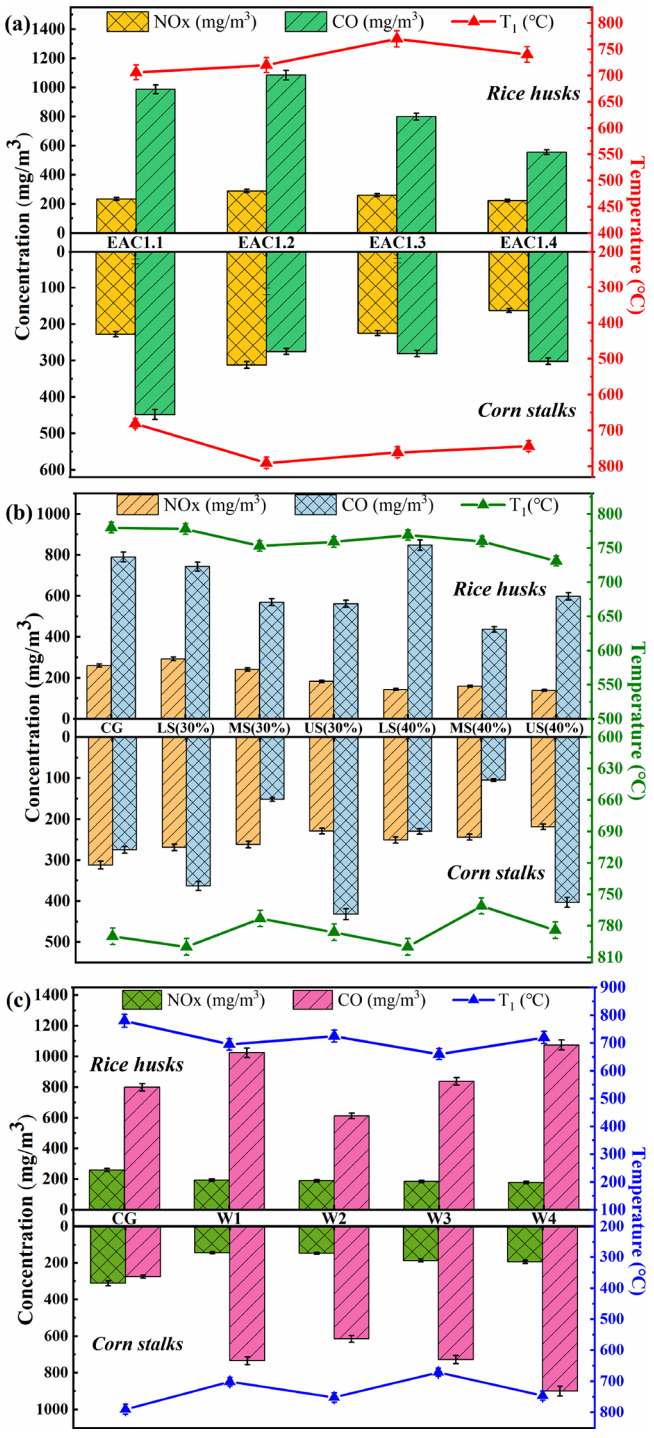

Figure 2. Variation diagram of NO_x and CO concentrations at fire outlet and temperature T_1. (a) Different excess air coefficients. (b) Ratios of secondary air to the total air volume at different heights. (c) Ratios of secondary air in different layers.

that position, which means that considerable variations in measured temperature can be obtained.

Following the comparison of the operating conditions EAC1.1−EAC1.4 during the rice husk burning, we select the staged air distribution combustion test at EAC1.3 for subsequent analysis. Under this condition, as the proportion of the secondary air in the total air volume increases (from 30% to 40%), the NO_x emission concentration is significantly reduced. This is consistent with the results of previous work.[32] When the secondary air equals 30% of the total air volume, NO_x emissions exhibit a significant reduction with the increasing secondary air height, from 300 mg/m^3 of LS (30%) to 180 mg/m^3 of US (30%). However, no significant changes are observed in the NO_x emissions at 40%, with values remaining close to 150 mg/m^3. The reduction effect is obvious, and the variation in the secondary air height under the condition of primary and secondary air classification (40%) has a limited impact on the NO_x emission concentration. Under the four secondary air multilayer air distributions, the NO_x emission concentration at the outlet during combustion does not change greatly, with values at around 180 mg/m^3 (Figure 2c). The outlet NO_x emissions in the primary and secondary air distribution combustion conditions exceed those of CG (with the exception of LS (30%)), while other operating conditions are reduced (Figure 2b). Rice husks also have lower NO_x emissions. However, under the multilayer secondary air distribution combustion condition, NO_x emissions during the rice husk combustion are similar to those under the primary secondary air staged distribution combustion outlet.

Figure 2 depicts the NO_x and CO concentrations and combustion zone temperature T_1 of the corn stalks under different air distribution conditions. In the absence of a graded air distribution, the CO emissions initially decrease and then subsequently increase with the increasing excess air coefficient (Figure 2a), differing to the results of Liu et al.[33] This can be explained by the relatively small amount of air entering the combustion chamber at the EAC1.1, with the insufficient amount of oxygen causing insufficient combustion and emitting more CO.[34] At the same time, due to insufficient oxygen, temperature T_1 at the lower part of the combustion chamber is relatively low. At EAC1.2 and EAC1.3, as the excess air coefficient increases, the fuel is fully combusted in the combustion chamber, and the generated CO and sufficient oxygen will undergo an oxidation reaction to form CO_2. Therefore, CO concentrations under these two combustion conditions are relatively low, and temperature T_1 is relatively high. However, note that the corresponding NO_x concentration at the fire outlet is also relatively high. As the excess air coefficient continues to increase, the inlet velocity of low-temperature air entering the combustion chamber from the lower part increases, which enhances the heat transfer rate inside the combustion chamber and shortens the flue gas residence time. This consequently reduces the internal combustion temperature and NO_x emission concentration. However, as the volatile matter stays in the combustion chamber for a short time period, the combustion is not complete, and the corresponding CO concentration increases.

The subsequent staged air distribution combustion test was performed at EAC1.2. At the primary and secondary air ratio of PA:SA = 70%:30%, the CO concentration increases under US (30%) and LS (30%) compared with CG (Figure 2b). Lower CO emissions are observed under MS (30%). This indicates that a suitable secondary air height will significantly reduce the CO concentration in the flue gas and facilitate the combustion process. In addition, distributing the primary and secondary air can reduce the NO_x concentration of the vent, with a decreasing trend as the height of the secondary air increases. Similar trends in the CO and NO_x concentrations at the vent are observed for the primary and secondary air ratio of 60%: 40%. As the secondary air height increases, CO concentrations initially decrease and subsequently increase, while NO_x concentrations gradually decrease. For CO

https://doi.org/10.1021/acsomega.2c02587
ACS Omega 2022, 7, 28962−28973

emissions, the difference caused in the pre-combustion period is relatively minor. The main difference might be attributed to the oxidation reaction of CO with O_2 to form CO_2 in the high temperature region of the main combustion. Therefore, the minor differences of T_1 obtained under LS (40%), MS (40%), and US (40%) are in the range of 45 °C, which indicates that the oxidation reaction dominated by the flue gas displacement plays a decisive role. However, MS (40%) is less efficient for flue gas replacement of the generated volatiles and CO. MS (40%) is more likely to maintain CO in the main combustion high temperature zone in the middle of the furnace and below. The oxidation reaction is also easier, resulting in a lower CO concentration at the outlet. However, CO and NO_x emissions are lower for the primary and secondary air ratio of 60%:40% compared to those at 70%:30%.

CO emissions in the flue gas under the four secondary air multilayer air distribution conditions are very high, reaching 900 mg/m^3 (Figure 2c). It is obvious that W_3 represents the condition with the strongest secondary air stage, while the W_4 condition represents the condition with the weakest secondary air stage. Therefore, the combustion should be correspondingly sufficient under W_3. In addition, for such a secondary air position, the generated CO is more likely to stay in the high temperature zone of the main combustion and undergo an oxidation reaction with O_2 to reduce the CO concentration. However, the temperature T_1 will decrease accordingly due to the increase in the heat transfer rate. The theoretical combustion efficiency decreases under W_4, but the appropriate excess air coefficient makes the combustion efficiency slightly lower than that of W_3, and the CO concentration increases accordingly. However, the air distribution of W_4 allows the heat transfer efficiency to dominate and the resulting CO is less likely to remain in the high temperature zone of the main combustion for oxidation reactions, resulting in a higher CO concentration than W_3. In contrast, NO_x concentrations are low, with a minimum close to 140 mg/m^3. This indicates the opposing change trends of CO and NO_x concentrations in the flue gas, which is consistent with previous research.[22] In summary, NO_x concentrations in the fire outlet are reduced across all secondary air multilayer distributions compared with the two control groups, while CO concentrations are increased. Biomass has comparable nitrogen content to coal but almost no sulfur. Therefore, the biomass combustion device hardly needs to install desulfurization equipment. As for the emissions of NO_x, after staged air distribution combustion of biomass, the NO_x emission concentration we obtained is lower than that of coal combustion under optimal conditions (350−250 mg/m^3). In summary, the optimized staged air distribution combustion of biomass presents a greater advantage than coal combustion in terms of controlling NO_x emissions.

3.2. NO_x Reduction Rate of Straw Pellet Combustion.

The NO_x reduction rate (η_N) was used to determine the degree of reduction in the NO_x concentrations under rice husk combustion for each air distribution condition compared with the CG. The larger the value of η_N, the greater the degree of NO_x reduction, that is, the lower the NO_x concentrations and the better the effect. η_N is calculated as follows:

$$\eta_N = \frac{NO_x(CG) - NO_x(y)}{NO_x(CG)} \times 100\% \quad (4)$$

where $NO_x(CG)$ is the NO_x concentration in CG; $NO_x(y)$ is the NO_x concentration obtained when the primary and secondary air is divided into different levels and the secondary air is multilayered; and y refers to US (30%), MS (30%), LS (30%), US (40%), MS (40%), LS (40%), W_1, W_2, W_3, and W_4.

Figure 3 shows the NO_x reduction rate of rice husks and corn stalks under different combustion conditions. NO_x

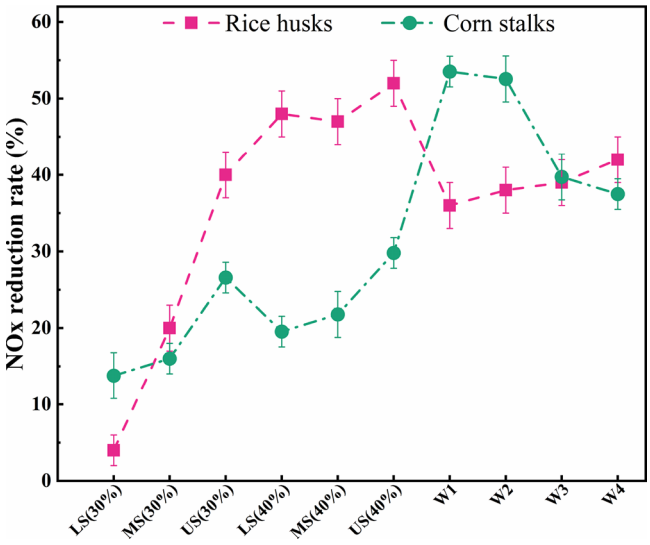

Figure 3. NO_x reduction rate under different combustion conditions.

emissions from rice husk combustion are minimized when the secondary air accounts for 40% of the total air volume, with a NO_x reduction rate close to 50% (Figure 3). At 30%, the NO_x reduction rate increases significantly with the secondary air height, yet this is not true at 40%. Under the multilayer secondary air distribution, the overall level of NO_x reduction rate ranges between 36% and 41%, with minimal variation. For the combustion of corn stalks at the EAC1.2, the use of the primary and secondary air graded air distribution can effectively reduce NO_x concentrations in the flue gas compared with just applying the primary air. The NO_x reduction rate exceeds 14% under this scenario (Figure 3). Note that irrespective of the secondary air height in the upper, middle, and lower layers, when the primary and secondary air ratio is 60%:40%, the NO_x reduction rate exceeds that of the PA:SA at 70%:30%. This demonstrates that the proportion of the secondary air in the total air volume is enhanced, helping to reduce the NO_x concentration in the flue gas. In addition, applying multilayered secondary air can further reduce the NO_x concentration, with a NO_x reduction rate between 38% and 53% and an obvious NO_x reduction effect. In particular, the NO_x reduction rates of W_1 and W_2 are significantly higher than those of W_3 and W_4.

Note that under the multilayer secondary air distribution combustion conditions, the NO_x emission concentration during the burning of rice husks is similar to that of corn stalk burning. However, the NO_x reduction effect is not obvious compared with the corn stalk combustion.

3.3. Characteristics of the Furnace Temperature Distribution.

The results in Section 3.2 reveal that the reduction in the NO_x emissions of rice husk combustion under the multilayer secondary air distribution is not obvious compared with that of corn stalks. Therefore, the outlet of the multilayer secondary air distribution combustion condition exhibits higher NO_x emissions for the combustion of rice husks and corn stalk fuel. NO content accounts for more than 90% of

https://doi.org/10.1021/acsomega.2c02587
ACS Omega 2022, 7, 28962−28973

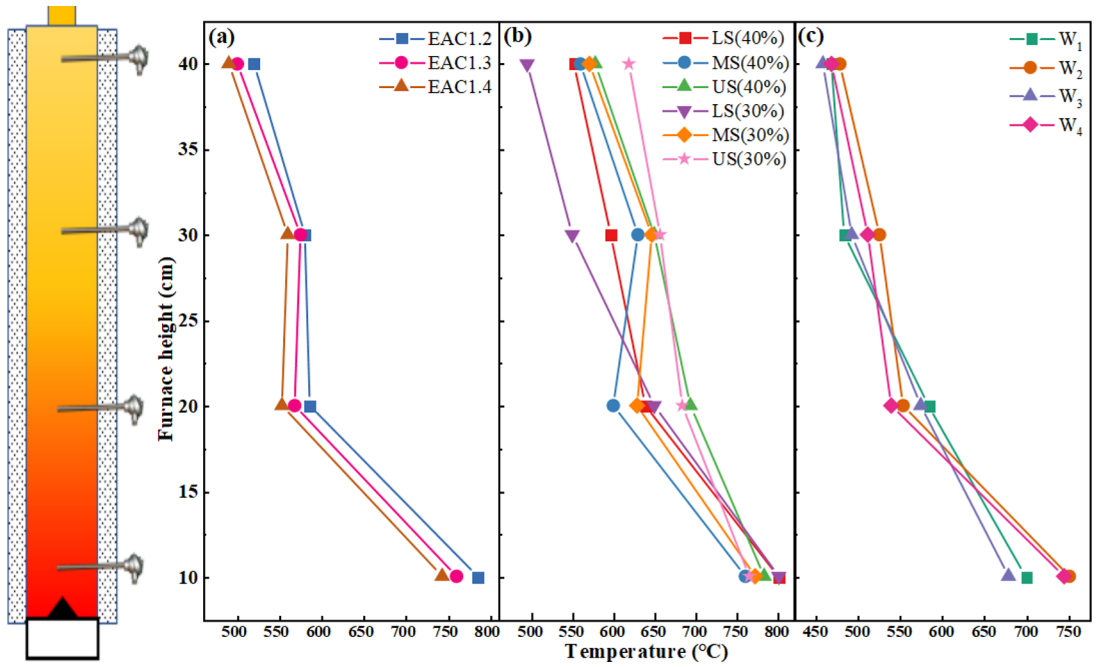

Figure 4. Temperature distribution in the combustion chamber of corn stalks. (a) Different excess air coefficients. (b) Ratio of secondary air to total air volume at different heights. (c) Different layer secondary air ratio.

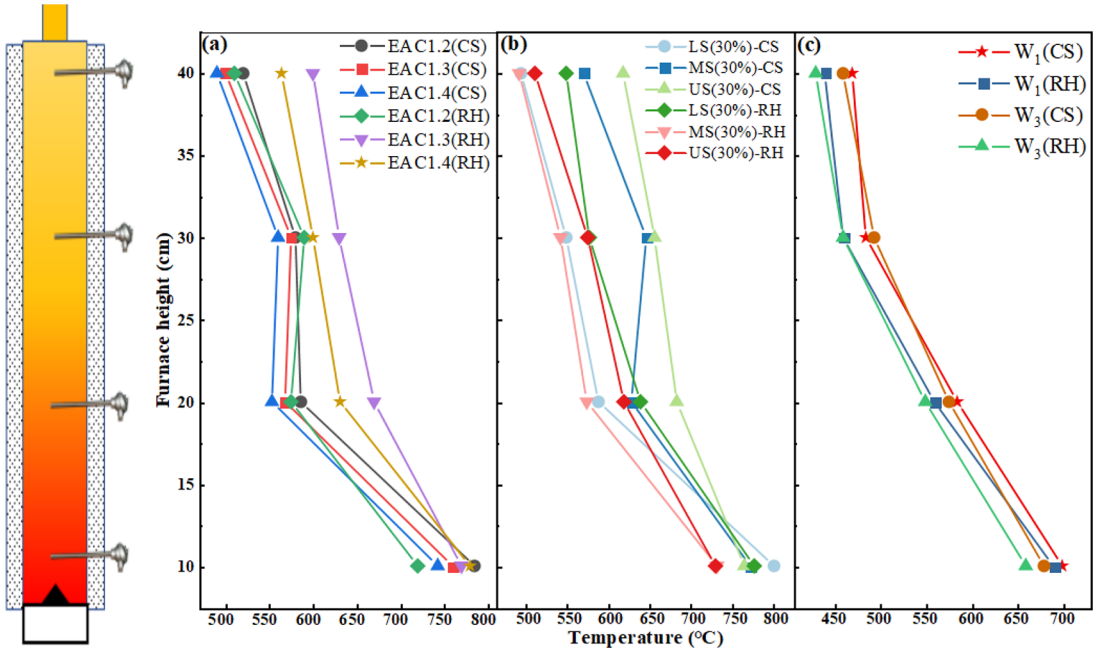

Figure 5. Temperature comparison between rice husk and corn stalk combustion chambers. (a) Different excess air coefficients. (b) Ratio of secondary air to total air volume at different heights. (c) Different layer secondary air ratio. Note: CS refers to corn stalks, and RH refers to rice husks.

NO_x, and the production of NO is closely related to the furnace temperature during combustion. In order to further investigate the high NO_x emissions during combustion, temperature measurement points were set at heights of 10, 20, 30, and 40 cm above the grate. We monitored and analyzed the internal temperature during combustion and selected the temperature data of different furnace heights in the stable combustion stage. This data was employed to calculate the average temperature value, allowing us to evaluate the subsequent reduction of NO_x emission concentrations. Figure 4 presents the temperature measurement points of corn stalks along the height of the combustion test bench.

Under the application of just primary air, the furnace temperature is observed to change for excess air coefficients of 1.2, 1.3, and 1.4 (Figure 4a). The temperature changes at different combustion chamber heights follow the same trend. More specifically, the temperature decreases as the measuring points increase. The lower the height of the measuring point, the more severe the temperature change. Moreover, increasing the excess air coefficient continues to decrease the temperature

https://doi.org/10.1021/acsomega.2c02587
ACS Omega 2022, 7, 28962−28973

Table 4. Heat Loss and Combustion Efficiency of Corn Stalks and Rice Husks under Different Working Conditions[a]

	carbon content/%		CO/%		q_1/%		q_2/%		η_c/%	
	CS	RH	CS	RH	CS	RH	CS	RH	CS	RH
EAC1.1	3.70	7.76	0.056	0.123	0.215	0.512	0.726	2.382	99.05	97.11
EAC1.2	3.40	7.46	0.034	0.148	0.130	0.616	0.665	2.269	99.20	97.12
EAC1.3	3.30	7.32	0.033	0.112	0.126	0.467	0.645	2.216	99.22	97.32
EAC1.4	3.30	6.84	0.037	0.044	0.142	0.185	0.645	2.037	99.21	97.78
LS(40%)	3.33	6.86	0.029	0.106	0.111	0.441	0.651	2.045	99.23	97.51
MS(40%)	3.35	6.86	0.014	0.054	0.053	0.227	0.655	2.046	99.29	97.73
US(40%)	3.50	7.31	0.050	0.075	0.192	0.311	0.685	2.209	99.12	97.48
W_1	3.45	8.21	0.091	0.128	0.349	0.532	0.675	2.549	98.97	96.92
W_2	3.60	8.24	0.077	0.076	0.295	0.318	0.706	2.564	98.99	96.12
W_3	3.50	8.32	0.110	0.105	0.422	0.436	0.686	2.595	98.89	95.97
W_4	3.20	8.12	0.090	0.134	0.345	0.559	0.625	2.528	99.02	95.92

[a]The value of CO is obtained by converting mg/m^3 to units in %.

of each measuring point accordingly. When the excess air coefficient is 1.2, compared with just the primary air distribution, applying the graded air distribution of the primary and secondary air results in the gradual decrease of temperature T_1 as the position of the secondary air entering the combustion chamber increases, while temperatures T_2, T_3, and T_4 increase significantly (Figure 4b). Increasing the height of the secondary air entrance will form a relatively oxygen-deficient area at the bottom of the combustion chamber, resulting in a reduction in the combustion temperature of the fuel. In addition, for both primary and secondary air ratios 60%:40% and 70%:30%, T_3 exceeds T_2 when the secondary air enters the center of the combustion chamber. This is attributed to the incomplete burning of part of the volatile matter in the principle combustion zone at the bottom of the combustion chamber. Due to the addition of the secondary air, the unburned volatile matter is fully burned here, and temperature T_3 rises. Compared with CG, under the four secondary air multilayer air distribution modes (W_1, W_2, W_3, and W_4), the temperature of each measurement point in the combustion chamber is reduced (Figure 4c). The temperature changes at T_1 and T_4 are most obvious, which is also a key influencing factor of the NO_x concentration reduction in the flue gas. This is a key advantage brought by the use of the secondary air multilayer air distribution, yet an excessively low temperature in the combustion chamber may impact the combustion efficiency of the corn stalks.

Figure 5 presents the temperature distribution characteristics at different heights in the furnace during the burning of rice husks and corn stalks. The temperatures T_2, T_3, and T_4 during rice husk burning exceed those of the corn stalk burning (Figure 5a). The opposite is true under the primary and secondary air staged combustion conditions (Figure 5b). The primary air is the main source of oxygen required for combustion in the furnace. It is the basis for stable combustion in the furnace and plays a key role in the combustion of volatile in the biomass. Compared with corn stalk, the pre-combustion process of rice husk is slower. When the secondary air enters the furnace from different positions, a relatively oxygen-deficient area is gradually formed at the bottom of the combustion chamber, and the combustion stability of rice husk is not as good as that of corn stalk. Therefore, the combustion temperature of rice husk is slightly lower than that of corn stalk. This is mainly due to the change in the combustion conditions of rice husk and corn stalk after the entry of secondary air. However, the temperatures of corn stalk and rice husk burning are generally similar, with temperature differences between T_1 and T_4 in all working conditions ranging within 100−200 °C. Note that T_3 is higher than T_2 in the MS (30%) working condition during the burning of corn stalks. This is due to the change in corn stalk burning conditions following the entry of the secondary air. Under burning conditions W_1 and W_3, the burning temperature of corn stalks at different heights exceeds that of rice husks by approximately 40 °C (Figure 5c). The combustion temperature change trends of the two fuels at different heights are consistent.

3.4. Combustion Efficiency of Straw Pellets. The heat loss and combustion efficiency of rice husk pellet combustion under different air distribution conditions were calculated using eqs 1−4 (Table 4). At EAC1.1, the combustion efficiency of corn stalks is low, reaching just 99.05%, while at EAC1.2−EAC1.4, the combustion efficiency exhibits a narrow range of 99.20%−99.22%. Compared with CG with only primary air, the combustion efficiency of corn stalks gradually decreases as the position of the secondary air entering the combustion chamber increases at EAC1.2. When the secondary air enters from the uppermost layer, the combustion efficiency is reduced to 99.12%. The combustion efficiency is further reduced under the four secondary air multilayer distribution modes (W_1, W_2, W_3, and W_4), with W_3 exhibiting the greatest reduction to 98.89%. This indicates that at high secondary air entrances or reduced lower secondary air volumes, the combustion of corn stalks can be incomplete, with a high carbon content in the ash, and a significant increase in CO emission concentrations. In addition, the temperature at the bottom of the combustion chamber decreases, thus reducing the combustion efficiency.

Table 4 reveals the combustion efficiency to be inversely proportional to the bottom ash carbon content. The CO emissions of the designed combustion test bench range between 0.04% and 0.16%, while the bottom ash carbon content is between 5.5% and 7.5%. For general biomass pellet burners, the combustion efficiency exceeds 95%,[35] which is mainly due to the characteristics of rice husk fuel and its inability to burn out readily. The combustion test results of the combustion test bench designed in this paper demonstrate a maximum combustion efficiency of 97.78% for rice husks as the fuel and generally a relatively good combustion effect. Under the combustion of straw biomass, the CO concentration and the bottom ash carbon content are key in determining the combustion efficiency. For rice husks, fuels with a high silicon content in ash require the design of a specific boiler for

https://doi.org/10.1021/acsomega.2c02587
ACS Omega 2022, 7, 28962−28973

Table 5. T_1 and Slagging Rate Corresponding to the Corn Stalk Combustion in Each Working Condition

working conditions	EAC1.2	EAC1.3	EAC1.4	LS(40%)	MS(40%)	W_1	W_2	W_3	W_4
T_1/°C	790	760	750	800	761	701	752	671	743
slagging rate/%	14.4	16	14.5	13	11.2	5	7.8	5.8	4.5

combustion research. In order to evaluate the degree of combustion and slagging of corn stalks under different air distribution conditions, we collected and weighed the burned ash and placed it on a SC-600 vibrating screen with a 6 mm screen for sieving for 30 s. After screening, the slag lump remaining on the screen was collected and weighed. The slagging rate (SR) is determined as follows:

$$C = \frac{G_1}{G_2} \times 100\% \quad \text{and SR} = \frac{G_1}{G_2} \tag{5}$$

SR is the slagging rate, %; G_1 is the slag with a pellet size greater than 6 mm, g; and G_2 is the total amount of ash formed, g.

Table 5 reports the fuel bed temperature T_1 and slagging rate of the corn stalk combustion chamber under different working conditions. Compared with CG, the slagging rate of the corn stalks exhibited a decreasing trend following the application of the primary and secondary air grading. This is particularly true when the secondary air enters the middle position of the combustion chamber (MS), with a reduction in the slagging rate by about 11.2%. When the secondary air multilayer air distribution is adopted, the slagging rate under the four working conditions (W_1, W_2, W_3, and W_4) is greatly reduced, and minimized under W_4 (4.5%). This is associated with the low temperature at the bottom of the combustion chamber at this time, and the addition of the secondary air multilayer air distribution has an impact on the gas phase release of elements such as K and Na in the ash at the bottom layer. The slagging rate of the corn stalks is highly correlated with temperature T_1 of the fuel bed. When T_1 is between 670−740 °C, the slagging rate is approximately 5%, while when T_1 is higher than 760 °C, the slagging rate will rapidly increase to over 11%. This indicates the key influencing role of T_1 in the combustion and slagging of corn stalks. Note that several air distribution conditions in Table 5 did not exhibit a higher temperature and slagging rate. Corn stalks are prone to severe ash slagging when burning, and NO_x emissions are high. Therefore, the NO_x emissions and ash slagging rate at the flue gas outlet are used as evaluation indicators to study the operating conditions for low NO_x emissions and slagging rates under corn stalk burning with air distribution conditions (Figure 6a). There is no slagging during rice husk combustion; thus, the export NO_x and CO emission concentrations are used as the evaluation index to select the optimal working conditions (Figure 6b).

During the burning of corn stalks, considering that various countries are implementing more stringent requirements for NO_x emission concentrations, the NO_x concentration is set as the key indicator for the selection of the optimal working conditions, and the lower slagging rate as the second indicator. From the test results, W_1 is considered to be the optimal air distribution condition for corn stalk combustion. If the low CO emission concentration in flue gas is considered as the selection standard, W_2 is the optimal condition. For general biomass boilers, the CO emission concentration is within 0.2%, while the CO emission concentration of the designed combustion test bed is between 0.04% and 0.16%, which is

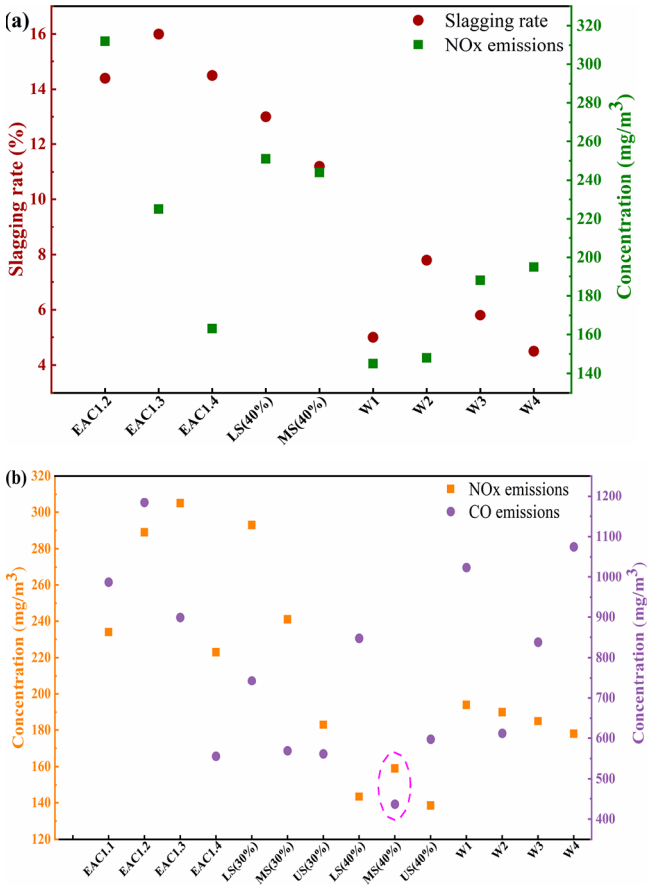

Figure 6. Analysis of optimal combustion condition of corn stalks (a) and rice husks (b).

lower than that of conventional biomass boilers. Among these operating conditions, only MS (40%) showed lower NO_x and CO emissions than 200 and 550 mg/m^3, respectively. More specifically, the outlet NO_x and CO emission concentrations simultaneously reach low levels, and thus MS (40%) is selected as the optimal air distribution condition.

3.5. Variations in the Ash and Inorganic Elements of Corn Stalks and Rice Husks. *3.5.1. Variations in the Ash and Inorganic Element Composition of Corn Stalks.* As a typical straw-like biomass, corn stalks not only produce higher NO_x emissions when burned, but the fuel layer is also prone to slagging,[36] seriously affecting the air distribution and burnout. Therefore, we focus on investigating the effect of different air distribution methods on the burning of corn stalks and slagging. The corn stalk ash and slag obtained from the combustion of the biomass pellet combustion test device are crushed, ground, and analyzed using a polycrystalline X-ray diffractometer (XRD, Bruker AXS D8 Advance, Germany). Figure 7 presents the variation of the main inorganic element content in the corn stalk ash with the combustion conditions.

The ash obtained from the combustion of corn stalks is in a soft state, relatively broken and has a low hardness level. However, the corn stalk residue is a glassy substance in

https://doi.org/10.1021/acsomega.2c02587
ACS Omega 2022, 7, 28962−28973

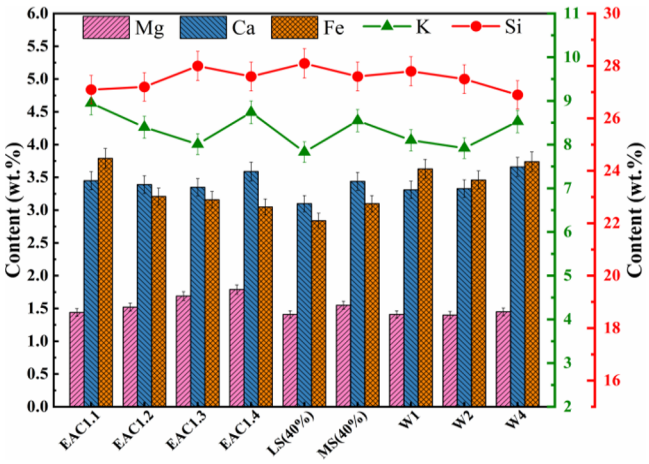

Figure 7. Change of element in ash from burning corn stalks.

appearance, with a high hardness, and the internal components of corn stalks that are not fully burned. As the Si content in the corn stalk raw materials accounts for approximately 5% of the total, a large amount of SiO_2 will be formed after combustion, and the K content is second only to the Si content. Therefore, there is a large amount of SiO_2 and KCl in the ash and slag from the combustion of corn stalks. When there is a local high temperature area in the combustion chamber, these two compounds easily form a low melting point co-crystal compound, and a large amount of slagging will be formed, complicating the air distribution and slag removal.[37] A large amount of slagging is caused by the high alkali metal element content in the bottom ash for the corn stalk combustion and the low alkaline earth metal element content (e.g., Ca and Mg). Therefore, we evaluate the elemental composition of the bottom ash of corn stalks under different combustion conditions. The Si content in the corn stalks ash exhibits minimal variations (between 24% and 26%). The Mg and Fe content change trends are opposing under each EAC1.1−EAC1.4 combustion condition, while the K and Ca content follow the same change trend.

The properties of ash are a function of its composition. At present, there is no suitable slagging judgment standard for different types of biomass combustion, and determining the slagging method of coal is the main reference point. Four commonly used slagging indexes were selected to analyze the combustion slagging tendency of corn stalks under different air distribution conditions. The silica ratio (G), alkali/acid ratio (B/A), Na content index (Na (index)), and alkaline index (Al_c) are calculated using formulas 6−9.[38]

Silica ratio (G):

$$G = \frac{SiO_2}{\text{equivalent } Fe_2O_3 + SiO_2 + MgO + CaO} \quad (6)$$

where equivalent $Fe_2O_3 = Fe_2O_3 + 1.11FeO + 1.43Fe$.

Alkali/acid ratio (B/A):

$$\frac{B}{A} = \frac{Fe_2O_3 + CaO + MgO + Na_2O + K_2O}{SiO_2 + Al_2O_3} \quad (7)$$

Na (index):

$$\text{Na (index)} = \frac{(Na_2O + 0.659K_2O)A_{ad}}{100} \quad (8)$$

Alkalinity index (Al_c):

$$Al_c = \frac{A(K_2O + Na_2O)\%}{LHV} \text{ and } Al_c = \frac{A_{ad}(Na_2O + K_2O)\%}{HHV} \quad (9)$$

where A_{ad} refers to the ash content of the fuel as air dried basis (wt %); HHV is high calorific value of fuel at dry base.

According to the inorganic element content of the slagging ash obtained under different air distribution conditions, four slagging prediction indexes can be calculated. The slagging index results in Table 6 are used to derive the relations of the four slagging indexes with temperature T_1. We combine the judgment range of each slagging index for analysis.[39,40] For silica ratio G, the slagging index reveals mild slagging, and G exhibits an upward trend with temperature T_1. Thus, the higher the temperature T_1, the less likely G is to form slag, which is contrary to the actual test data. For the alkali/acid ratio (B/A), the slagging index denotes moderate slagging, yet increasing temperature T_1 lowers the corresponding predicted slagging degree, which is also inconsistent with the actual situation. Similarly, the Na (index) and alkalinity index (Al_c) present serious slagging according to the slagging index, yet increasing temperature T_1 also lowers the corresponding predicted slagging degree. This is also inconsistent with the actual test results. Therefore, none of the above four slagging indexes can accurately predict the slagging tendency of different fuel areas based on the inorganic elements content in the slagging of corn stalk combustion under varying temperature T_1 changes. Note that the slagging rate of corn stalks is strongly related to temperature T_1. In addition, a high fitting degree is observed between G and temperature T_1 under different combustion conditions. Therefore, temperature T_1 is introduced as a variable in the silicon ratio G. Following several amendments, the formula is described as follows:

$$G_t = G \times 1.1 - T_1 \times 0.03\% \quad (10)$$

Figure 8 shows the modified predictive index (G_t) results when the temperature T_1 of the different combustion zone is calculated. As temperature T_1 in the combustion zone continues to increase, G_t exhibits a downward trend, enhancing the slagging tendency. When temperature T_1 is close to 800 °C, G_t is between 0.66 and 0.67 and denotes a severe slagging risk. At the T_1 temperature of 680 °C, the G_t value is relatively large, with a moderate slagging tendency. Therefore, the G_t can effectively predict the slagging tendency of corn stalks with

Table 6. Calculation Results of Four Slagging Prediction Indexes under Different Working Conditions

conditions	EAC1.1	W_1	EAC1.4	W_4	EAC1.3	MS(40%)	W_2	EAC1.2	LS40%
T_1(°C)	672	708	743	750	756	762	776	785	800
G	0.809	0.818	0.805	0.819	0.820	0.821	0.819	0.818	0.835
B/A	0.363	0.333	0.362	0.331	0.322	0.337	0.332	0.339	0.305
Na (index)	0.765	0.714	0.734	0.701	0.689	0.732	0.706	0.721	0.692
Al_c	0.660	0.610	0.632	0.603	0.593	0.631	0.602	0.621	0.591

https://doi.org/10.1021/acsomega.2c02587
ACS Omega 2022, 7, 28962−28973

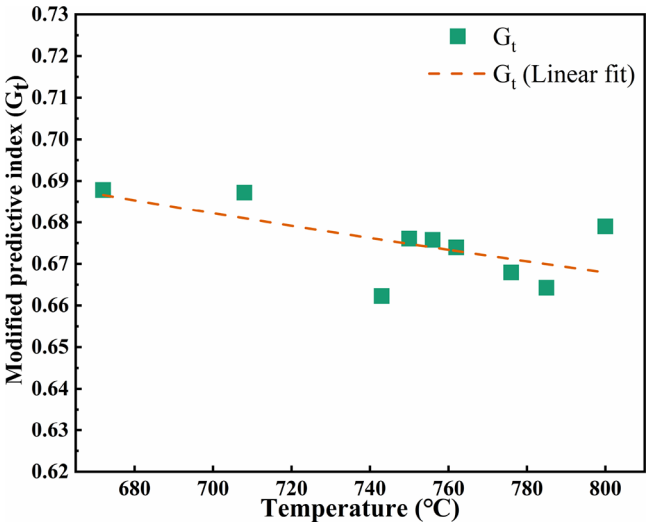

Figure 8. Graph of G_t results versus temperature T_1.

temperature T_1 and provides a basis for the prediction of slagging under secondary air multilayer combustion.

3.5.2. Variations of Inorganic Elements in the Rice Husk Ash. When rice husks are burned on the biomass combustion test bench, a large amount of black bottom ash is produced, irrespective of the working conditions. The production of black ash from rice husks is the result of unburned carbon.[31] The incomplete carbon combustion may be related to the relatively short combustion time and insufficient air contact. When the combustion test is performed on the combustion test bench, after a certain period of time, new fuel enters the furnace, causing the unburned rice husk ash to backlog to the bottom. In the subsequent combustion, the contact with air is not sufficient while at the same time the combustion time is not long enough for black ash to form. This is attributed to the special Si framework of rice husk ash, which prevents the diffusion combustion from proceeding and prolongs the burnout time. In addition, since the rice husk ash is totally dominated by Si, with a considerable lack of corresponding cation forming elements like K, Ca, Na, etc., the ash will be dominated by SiO_2 that do not form slag in the present conditions. This may explain why rice husks do not produce slagging when burning on the combustion test bench. Figure 9 depicts the varying content of several elements in rice husk ash under different working conditions.

The Si content exhibits limited variations in the rice husk ash (fluctuating around 40 ± 2%) under both an increasing excess air coefficient and varying primary and secondary air staged combustion conditions. This may be linked to the limited precipitation of the Si element when the rice husks are burned, with the majority remaining in the bottom ash.[41] The K percentage in rice husk ash is generally higher in the primary and secondary air staged air distribution combustion (Figure 9). This is caused by the lower temperature T_1 of the fuel layer during air staged combustion. Numerous studies[42,43] have proven that the amount of K precipitation increases with the combustion temperature and combustion heating rate. This is because during the pre-combustion stage when biomass volatiles are precipitated, the fuel will undergo pyrolysis and generate tar and light hydrocarbon compounds. The tar and light hydrocarbon compounds[44] will subsequently undergo a second pyrolysis under high temperature conditions and

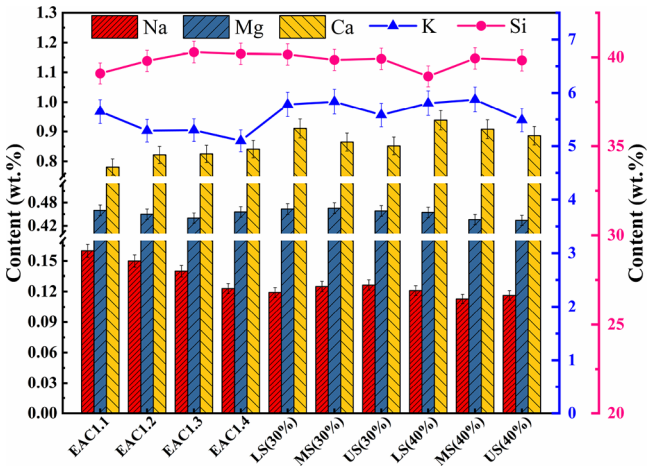

Figure 9. Change law of various elements in rice husks ash.

generate H-based free radicals. The chemical reaction between the H radical and char sample breaks the chemical bond between the carbon base and the alkali metal, resulting in the precipitation of the alkali metal element during the pyrolysis process. The chemical formula of the process is as follows:[45]

$$R + C - Y \rightarrow C - R + Y \quad (11)$$

where C is a carbon base; Y is an alkali metal substance; and R is a free radical.

In the volatilization analysis stage, the reaction temperature and resultant energy are low. This does not meet the conditions required to destroy most of the chemical bonds during the second pyrolysis, and thus the free radicals in the reaction are not easily formed. The reaction of formula 11 is inhibited to a certain extent, and the alkali metal does not have enough energy to break away from the carbon group and cannot be precipitated. Hence, the reaction temperature is very important for the precipitation of alkali metal elements during the combustion of biomass fuel.

4. CONCLUSIONS

(1) The use of multilayer secondary air distribution can significantly reduce the NO_x concentration for both corn stalks and rice husks. Compared with rice husks, the multilayer secondary air distribution exerts a more obvious reduction effect on the NO_x emission concentration of the corn stalk combustion. The CO and NO_x concentration changes in the flue gas are opposing, demonstrating a competitive relationship.

(2) The combustion slagging rate of corn stalks is highly correlated with the temperature of fuel layer T_1, which is an important factor affecting combustion slagging. When the NO_x concentration and slagging rate are used as the evaluation indicators for the optimal conditions of corn stalk combustion, W_1 is the optimal air distribution condition.

(3) The proposed G_t can effectively predict the slagging tendency of corn stalks with the combustion zone temperature T_1.

AUTHOR INFORMATION

Corresponding Author

Shanjian Liu − *School of Agricultural Engineering and Food Science, Shandong University of Technology, Zibo 255049,*

https://doi.org/10.1021/acsomega.2c02587
ACS Omega 2022, 7, 28962−28973

China; State Key Laboratory of Utilization of Woody Oil Resource, Zibo 255049, China; orcid.org/0000-0002-8756-9595; Email: liushanjian08@163.com

Authors

Zhisen He − *School of Agricultural Engineering and Food Science, Shandong University of Technology, Zibo 255049, China*

Shuaichao Wang − *School of Agricultural Engineering and Food Science, Shandong University of Technology, Zibo 255049, China*

Weidong Liu − *School of Agricultural Engineering and Food Science, Shandong University of Technology, Zibo 255049, China*

Yongjun Li − *School of Agricultural Engineering and Food Science, Shandong University of Technology, Zibo 255049, China; State Key Laboratory of Utilization of Woody Oil Resource, Zibo 255049, China*

Xiangdong Feng − *School of Agricultural Engineering and Food Science, Shandong University of Technology, Zibo 255049, China*

Complete contact information is available at: https://pubs.acs.org/10.1021/acsomega.2c02587

Notes

The authors declare no competing financial interest.

■ ACKNOWLEDGMENTS

The research was sponsored by National Natural Science Foundation of China (No.51606113), National Key Research and Development Program of China (No.2019YFD1100602) and SDUT & Zhoucun City Integration Development Project (No. 2020ZCXCZH09).

■ REFERENCES

(1) Saidur, R.; Abdelaziz, E. A.; Demirbas, A.; Hossain, M. S.; Mekhilef, S. A review on biomass as a fuel for boilers. *Renewable Sustainable Energy Rev.* **2011**, *15*, 2262−2289.

(2) Nunes, L. J. R.; Loureiro, L. M. E. F.; Sá, L. C. R.; Silva, H. F. C. Evaluation of the potential for energy recovery from olive oil industry waste: Thermochemical conversion technologies as fuel improvement methods. *Fuel* **2020**, *279*, No. 118536.

(3) Guo, F.; Zhong, Z. Co-combustion of anthracite coal and wood pellets: Thermodynamic analysis, combustion efficiency, pollutant emissions and ash slagging. *Environ. Pollut.* **2018**, *239*, 21−29.

(4) Balat, M.; Balat, H. Recent trends in global production and utilization of bio-ethanol fuel. *Appl. Energy* **2009**, *86*, 2273−2282.

(5) Cheng, W.; Zhu, Y.; Shao, J. a.; Zhang, W.; Wu, G.; Jiang, H.; Hu, J.; Huang, Z.; Yang, H.; Chen, H. Mitigation of ultrafine particulate matter emission from agricultural biomass pellet combustion by the additive of phosphoric acid modified kaolin. *Renewable Energy* **2021**, *172*, 177−187.

(6) Rebbling, A.; Näzelius, I.-L.; Schwabl, M.; Feldmeier, S.; Schön, C.; Dahl, J.; Haslinger, W.; Boström, D.; Öhman, M.; Boman, C. Prediction of slag related problems during fixed bed combustion of biomass by application of a multivariate statistical approach on fuel properties and burner technology. *Biomass Bioenergy* **2020**, *137*, No. 105557.

(7) Mlonka-Mędrala, A.; Magdziarz, A.; Gajek, M.; Nowińska, K.; Nowak, W. Alkali metals association in biomass and their impact on ash melting behaviour. *Fuel* **2020**, *261*, No. 116421.

(8) Wang, C. a.; Zhao, L.; Liu, C.; Gao, X.; Li, G.; Che, D. Comparative study on ash characteristics of various high-alkali fuels using different ashing methods and temperatures. *Fuel* **2021**, *299*, No. 120912.

(9) Gogolev, I.; Pikkarainen, T.; Kauppinen, J.; Linderholm, C.; Steenari, B.-M.; Lyngfelt, A. Investigation of biomass alkali release in a dual circulating fluidized bed chemical looping combustion system. *Fuel* **2021**, *297*, No. 120743.

(10) Qi, J.; Li, H.; Han, K.; Zuo, Q.; Gao, J.; Wang, Q.; Lu, C. Influence of ammonium dihydrogen phosphate on potassium retention and ash melting characteristics during combustion of biomass. *Energy* **2016**, *102*, 244−251.

(11) Paneru, M.; Babat, S.; Maier, J.; Scheffknecht, G. Role of potassium in deposit formation during wood pellets combustion. *Fuel Process. Technol.* **2016**, *141*, 266−275.

(12) Huang, L.; Zhu, Y.; Wang, Q.; Zhu, A.; Liu, Z.; Wang, Y.; Allen, D. T.; Li, L. Assessment of the effects of straw burning bans in China: Emissions, air quality, and health impacts. *Sci. Total Environ.* **2021**, *789*, No. 147935.

(13) Jiang, W.; Yan, T.; Chen, B. Impact of media channels and social interactions on the adoption of straw return by Chinese farmers. *Sci. Total Environ.* **2021**, *756*, No. 144078.

(14) Mu, L.; Li, T.; Wang, Z.; Shang, Y.; Yin, H. Influence of water/acid washing pretreatment of aquatic biomass on ash transformation and slagging behavior during co-firing with bituminous coal. *Energy* **2021**, *234*, No. 121286.

(15) Wang, W.; Wen, C.; Liu, T.; Li, C.; Xu, J.; Liu, E.; Liu, H.; Yan, K. Emission reduction of PM10 via pretreatment combining water washing and carbonisation during rice straw combustion: Focus on the effects of pretreatment and combustion conditions. *Fuel Process. Technol.* **2020**, *205*, No. 106412.

(16) Clery, D. S.; Mason, P. E.; Rayner, C. M.; Jones, J. M. The effects of an additive on the release of potassium in biomass combustion. *Fuel* **2018**, *214*, 647−655.

(17) Wang, Q.; Han, K.; Wang, P.; Li, S.; Zhang, M. Influence of additive on ash and combustion characteristics during biomass combustion under O2/CO2 atmosphere. *Energy* **2020**, *195*, No. 116987.

(18) Ma, W.; Zhou, H.; Zhang, J.; Zhang, K.; Liu, D.; Zhou, C.; Cen, K. Behavior of Slagging Deposits during Coal and Biomass Co-combustion in a 300 kW Down-Fired Furnace. *Energy Fuels* **2018**, *32*, 4399−4409.

(19) Li, H.; Chi, H.; Hu, S.; Wang, Y.; Song, G.; Abdulmajid, A. S.; He, L.; Wang, Y.; Su, S.; Xiang, J. Comprehensive study on intrinsic combustion behavior of non-premixed coal-biomass pellet at rapid heating rate. *Fuel* **2021**, *287*, No. 119496.

(20) Wang, Y.; Zhou, Y.; Bai, N.; Han, J. Experimental investigation of the characteristics of NOx emissions with multiple deep air-staged combustion of lean coal. *Fuel* **2020**, *280*, No. 118416.

(21) Liu, H.; Chaney, J.; Li, J.; Sun, C. Control of NOx emissions of a domestic/small-scale biomass pellet boiler by air staging. *Fuel* **2013**, *103*, 792−798.

(22) Fan, W.; Chen, J.; Feng, Z.; Wu, X.; Liu, S. Effects of reburning fuel characteristics on NOx emission during pulverized coal combustion and comparison with air-staged combustion. *Fuel* **2020**, *265*, No. 117007.

(23) Sher, F.; Pans, M. A.; Afilaka, D. T.; Sun, C.; Liu, H. Experimental investigation of woody and non-woody biomass combustion in a bubbling fluidised bed combustor focusing on gaseous emissions and temperature profiles. *Energy* **2017**, *141*, 2069−2080.

(24) Choi, M.; Kim, K.; Li, X.; Deng, K.; Park, Y.; Seo, M.; Sung, Y.; Choi, G. Strategic combustion technology with exhaust tube vortex flame: Combined effect of biomass co-firing and air-staged combustion on combustion characteristics and ash deposition. *Energy* **2020**, *203*, No. 117839.

(25) Kuang, M.; Wang, J.; Wang, X.; Zhao, X.; Chen, Y.; Du, L. In-furnace flow field, coal combustion and NOx emission characteristics regarding the staged-air location in a cascade-arch down-fired furnace. *J. Energy Inst.* **2021**, *98*, 259−270.

(26) Wang, D.; Liu, L.; Yuan, Y.; Yang, H.; Zhou, Y.; Duan, R. Design and key heating power parameters of a newly-developed

household biomass briquette heating boiler. *Renewable Energy* **2020**, *147*, 1371−1379.
(27) Bianco, V.; Szubel, M.; Matras, B.; Filipowicz, M.; Papis, K.; Podlasek, S. CFD analysis and design optimization of an air manifold for a biomass boiler. *Renewable Energy* **2021**, *163*, 2018−2028.
(28) Madhiyanon, T.; Sathitruangsak, P.; Sungworagarn, S.; Udomman, T. Investigation of rice-straw-ash fouling/slagging and countermeasures using supplementary additives and co-firing with Si−Al-rich coal in a pilot-scale grate-fired combustor. *J. Energy Inst.* **2020**, *93*, 1848−1867.
(29) Mack, R.; Kuptz, D.; Schön, C.; Hartmann, H. Combustion behavior and slagging tendencies of kaolin additivated agricultural pellets and of wood-straw pellet blends in a small-scale boiler. *Biomass Bioenergy* **2019**, *125*, 50−62.
(30) Boström, D.; Skoglund, N.; Grimm, A.; Boman, C.; Öhman, M.; Broström, M.; Backman, R. Ash Transformation Chemistry during Combustion of Biomass. *Energy Fuels* **2011**, *26*, 85−93.
(31) Krishnarao, R. V.; Subrahmanyam, J.; Jagadish Kumar, T. Studies on the formation of black particles in rice husk silica ash. *J. Eur. Ceram. Soc.* **2001**, *21*, 99−104.
(32) Zhu, T.; Hu, Y.; Tang, C.; Wang, L.; Liu, X.; Deng, L.; Che, D. Experimental study on NOx formation and burnout characteristics of pulverized coal in oxygen enriched and deep-staging combustion. *Fuel* **2020**, *272*, No. 117639.
(33) Liu, H.; Qiu, G.; Shao, Y.; Riffat, S. B. Experimental investigation on flue gas emissions of a domestic biomass boiler under normal and idle combustion conditions. *Int. J. Low-Carbon Technol.* **2010**, *5*, 88−95.
(34) Gungor, A. Analysis of combustion efficiency in CFB coal combustors. *Fuel* **2008**, *87*, 1083−1095.
(35) Pradhan, P.; Mahajani, S. M.; Arora, A. Production and utilization of fuel pellets from biomass: A review. *Fuel Process. Technol.* **2018**, *181*, 215−232.
(36) Chen, C.; Bi, Y.; Huang, Y.; Huang, H. Review on slagging evaluation methods of biomass fuel combustion. *J. Anal. Appl. Pyrolysis* **2021**, *155*, No. 105082.
(37) Fernández, M. J.; Mediavilla, I.; Barro, R.; Borjabad, E.; Ramos, R.; Carrasco, J. E. Sintering reduction of herbaceous biomass when blended with woody biomass: predictive and combustion tests. *Fuel* **2019**, *239*, 1115−1124.
(38) Barroso, J.; Ballester, J.; Pina, A. Study of coal ash deposition in an entrained flow reactor: Assessment of traditional and alternative slagging indices. *Fuel Process. Technol.* **2007**, *88*, 865−876.
(39) Niu, Y.; Tan, H.; Wang, X.; Liu, Z.; Liu, H.; Liu, Y.; Xu, T. Study on fusion characteristics of biomass ash. *Bioresour. Technol.* **2010**, *101*, 9373−9381.
(40) Lolja, S. A.; Haxhi, H.; Dhimitri, R.; Drushku, S.; Malja, A. Correlation between ash fusion temperatures and chemical composition in Albanian coal ashes. *Fuel* **2002**, *81*, 2257−2261.
(41) Ogwang, G.; Olupot, P. W.; Kasedde, H.; Menya, E.; Storz, H.; Kiros, Y. Experimental evaluation of rice husk ash for applications in geopolymer mortars. *J. Bioresour. Bioprod.* **2021**, *6*, 160−167.
(42) He, Z.; Lou, C.; Fu, J.; Lim, M. Experimental investigation on temporal release of potassium from biomass pellet combustion by flame emission spectroscopy. *Fuel* **2019**, *253*, 1378−1384.
(43) Liu, Y.; Wang, Z.; Xia, J.; Vervisch, L.; Wan, K.; He, Y.; Whiddon, R.; Bahai, H.; Cen, K. Measurement and kinetics of elemental and atomic potassium release from a burning biomass pellet. *Proc. Combust. Inst.* **2019**, *37*, 2681−2688.
(44) He, W.; Yin, G.; Zhao, Y.; Zhang, L.; Xu, S.; Huang, T.; Chang, L.; Lu, H. Interactions between free radicals during co-pyrolysis of lignite and biomass. *Fuel* **2021**, *302*, No. 121098.
(45) Jiang, L.; Hu, S.; Xiang, J.; Su, S.; Sun, L.; Xu, K.; Yao, Y. Release characteristics of alkali and alkaline earth metallic species during biomass pyrolysis and steam gasification process. *Bioresour. Technol.* **2012**, *116*, 278−284.

https://doi.org/10.1021/acsomega.2c02587
ACS Omega 2022, 7, 28962−28973